Electron-dependent thermoelectric properties in $Si/Si_{1-x}Ge_x$ heterostructures and $Si_{1-x}Ge_x$ alloys from first-principles

M. Z. Hossain[1,a)] and H. T. Johnson[2]
[1]*Division of Engineering and Applied Science, California Institute of Technology, Pasadena, California 91125, USA* .
[2]*Department of Mechanical Science and Engineering, University of Illinois at Urbana-Champaign, Urbana, Illinois 61801, USA*

(Received 9 April 2012; accepted 1 June 2012; published online 18 June 2012)

Unlike phononic thermal conductivity (which is shown in the literature to be reduced due to alloying and has a nearly constant value over a range of compositional variations), electron-dependent thermoelectric properties are shown here, from first-principles, to vary nonlinearly with composition. Of the $Si/Si_{1-x}Ge_x$ systems considered, the maximum thermopower observed, which is 10% higher than that of crystalline Si, is obtained for a $Si_{0.875}Ge_{0.125}$ alloy. Also, heterostructuring is shown to reduce thermopower, electrical conductivity, and electron thermal conductivity. Additionally, neither Lorenz number nor Seebeck coefficient shows oscillations for heterostructures, regardless of electron/hole energies, contradicting the conclusions obtained with miniband approximations. © *2012 American Institute of Physics.* [http://dx.doi.org/10.1063/1.4729765]

The thermoelectric figure of merit or ZT,[1–5] which is defined as $S^2T\sigma/(\kappa^e + \kappa^l)$, where S, σ, κ^e, κ^l are the Seebeck coefficient or thermopower, electrical conductivity, electron thermal conductivity, and lattice or phonon thermal conductivity, respectively, characterizes the efficiency of a thermoelectric material and involves transport of electrons as well as phonons. To enhance ZT, phononic properties must be altered to reduce the thermal conductivity, and electronic properties must be altered to maximize the thermopower and electrical conductivity. However, due to the complexity of optimizing several interdependent phononic and electronic properties simultaneously, it remains a challenge to find a combination of the properties or to find mechanisms that would provide promising values of ZT.

Although both experimental[6–9] and theoretical efforts[10–13] have focused on finding ways to enhance ZT in different material/design conditions, accurate determination of electronic and phononic contributions and their dependence on alloy composition, strain, or nanostructuring, particularly on the nanoscale, continues to be a formidable task. While experimentally it is difficult to carry out transport measurements, particularly on the nanoscale,[5,13] theoretical studies,[13–16] mostly use a finite number of bands to estimate the electronic contribution. In these methods, using parabolic or non-parabolic dispersion relations for computing the effective mass of electrons, local strain-induced charge effects on band bending at the heterointerface are disregarded. Consequently, contradictory conclusions for the same system are reported. For example, unlike single band calculations,[14,15] multiple-miniband calculations[13,16] show oscillatory behavior for the Seebeck coefficient and the Lorenz number (which is proportional to the ratio between κ^e and σ).

On the other hand, first-principles based transport calculation methods (which do not have any approximations and serve as the most accurate method, though with a high computational cost) incorporate a complete description of the electronic bands and have been used to find electron dependent transport properties and mechanisms accurately, for a range of electronic materials.[17–19] Using a combination of density functional theory (DFT) and the Boltzmann transport equation, we study the $Si/Si_{1-x}Ge_x$ system (which holds particular importance in widely used Si-based technologies and offers high ZT values, particularly at high temperatures[4]) as a model for determining the role of alloying and heterostructuring on its electron dependent transport properties. We find that neither S nor L shows oscillations regardless of electron energies, contradicting the conclusions obtained with limited number of bands.[13] Furthermore, in the literature, effects of low dimensionality and alloying on phononic contributions have been studied extensively for $Si/Si_{1-x}Ge_x$ systems[7,8] and significant improvements on ZT have been suggested. In this work, focusing on electron transport, we show that alloying offers much higher enhancement on electron dependent thermoelectric properties compared to heterostructuring, which is different than how phonon dependent properties behave in similar conditions. We also show that the maximum possible thermopower for this material system occurs for a germanium fraction of 12.5%, suggesting the best possible alloy composition for enhancing the thermoelectric figure of merit.

The electronic effects are investigated with three different atomic configurations: (1) alloy configuration (denoted by SiGe) to study the effect of compositional variation alone, (2) heterostructure configuration with pure Si on one side and Ge on other (denoted by Si/Ge) to study the effect of heterostructure formation alone, and (3) a combination thereof (denoted by Si/SiGe) to study the combined effect of alloying and heterostructuring. The supercell for the alloy configuration contains 64 atoms, and the nanostructure configuration contains 48, 64, or 80 atoms, as shown in Fig. 1. For the heterostructure configuration, only one unit cell is taken along the transverse directions, the y and z-directions. This introduces local-ordering along the lateral directions, but its effect on transport coefficients is found to be negligible. The total number of unit cells, $(m+n)$ along the

a)E-mail: zubaer@caltech.edu.

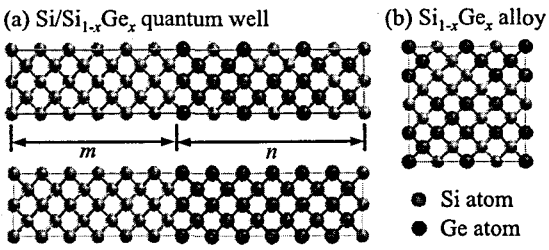

FIG. 1. Atomistic configurations: (a) $Si/Si_{1-x}Ge_x$ heterostructure configuration, (b) $Si_{1-x}Ge_x$ alloy configuration. The lengths of crystalline Si and alloy $Si_{1-x}Ge_x$ parts in (a) are denoted by "m" and "n," respectively. The total length of the superlattice is $(m+n)$. For studying the effect of alloying alone, the configuration (b) containing 64 atoms is used, and for the effect of nanostructuring alone, the configuration shown in (a) is used. To study the effect of compositional variation, Ge fraction is varied from $x=0$ to 1.0 with an interval of 0.125 in (b), and for the lower figure in (a) $x=0$, which gives a Si/Ge crystalline superlattice configuration; and for the upper figure in (a) $x=0.125$, 0.25, 0.5, and 0.75.

longitudinal direction is 6, 8, or 10 with $x=0.25$, 0.5, and 0.75 fraction of Ge atoms in the n-cells. In studying the effect of nanostructuring alone, m unit cells of Si and n unit cells of Ge are considered. Keeping $(m+n)$ fixed, $(m{:}n)$ is varied such that the effects of the length ratio can be studied. On the other hand, for studying the combined effects of alloying and heterostructuring, we consider m unit cells of Si and n unit cells of $Si_{1-x}Ge_x$ taking $m=n$. Due to an exponential increase in the computational cost, the simulations are carried out for a maximum of 10 unit cells along the longitudinal direction containing 80 atoms with a length scale of 5.5 nm. The lattice parameters for Si/Ge or Si/SiGe heterostructures are computed according to Eqs. (1) and (2)

$$a_{\parallel} = \frac{a_{Si}G_{Si}h_{Si} + a_{Ge}G_{Ge}h_{Ge}}{G_{Si}h_{Si} + G_{Ge}h_{Ge}}, \tag{1}$$

$$a_{\perp} = a(x)\left[1 - \frac{2C_{12}(x)}{C_{11}(x)}\left(\frac{a_{11}}{a(x)} - 1\right)\right], \tag{2}$$

where, $a_{\parallel}$, $a_{\perp}$ are the in-plane and out-of-plane lattice parameters, respectively, $a(x)$ is the composition dependent equilibrium lattice constant of $Si_{1-x}Ge_x$, C_{11} and C_{12} are elastic constants, and G is the shear modulus. Formation of interface and random positioning of the constituent atoms, particularly in the alloy configuration, introduce strain in the supercell and affect band potential across the heterointerface.[25–29] For a short-period superlattice, the former effect can make the microscopic average of the band potential vary sinusoidally over the supercell, with its wavelength being approximately equal to the width of the superlattice. First-principles calculations focused on this particular point illustrate the complex behavior of the band potential and the associated charge distribution, which are usually not incorporated in miniband calculations in a rigorous manner. Consequently, the constant band potential approximation, especially for short-period superlattices, may lead to spurious effects in band bending calculations.

Electronic structure calculations are performed using the density functional theory code SIESTA,[20] within the generalized gradient approximation for the exchange-correlation energy. Convergence of the total energy is achieved for a Monkhorst-Pack k-mesh of $(k_x, k_y, k_z) \equiv (2\times2\times2)$ and $(1\times8\times8)$ for the alloy and nanostructure configurations, respectively. Constructed atomistic configurations are relaxed using a Broyden scheme with a force tolerance of 1 mRy/bohr[3] to remove disorder or local strain induced forces at the interface or in the bulk. Transport properties are computed following the procedure outlined in Refs. 1 and 21 and incorporating energy dependent relaxation time functions. Using the explicit forms given by Mohan and Sofo,[1] the electron dependent transport coefficients are transformed into the following tensor form:

$$S_{\alpha\beta} = \frac{\int \frac{\partial f_0}{\partial E}\Xi_{\alpha\beta}(E-E_f)dE}{eT\int \frac{\partial f_0}{\partial E}\Xi_{\alpha\beta}dE}, \tag{3}$$

$$\sigma_{\alpha\beta} = -e^2\int \frac{\partial f_0}{\partial E}\Xi_{\alpha\beta}dE, \tag{4}$$

$$\kappa^e_{\alpha\beta} = -\frac{1}{T}\int \frac{\partial f_0}{\partial E}\Xi_{\alpha\beta}(E-E_f)^2dE, \tag{5}$$

$$\frac{\partial f_0}{\partial E} = -\frac{\left(\frac{1}{k_BT}\right)\exp\frac{E-E_f}{k_BT}}{\left(\exp\frac{E-E_f}{k_BT}+1\right)^2}, \tag{6}$$

$$\Xi_{\alpha\beta} = \sum_k \tau(E)v_\alpha(k)v_\beta(k)\delta(E-E_k), \tag{7}$$

where, f_0 is Fermi distribution function, T is the temperature, E is the energy, Ξ is the energy dependent transmission function, and k_B is the Boltzmann constant, σ is the electrical conductivity, ν is the electron group velocity, and κ^e is the electron thermal conductivity, and α and β are indices representing the tensor components. The transmission function is expressed as a function of energy, $\tau(E)=\alpha(E-E_f)^n$, where the exponent n depends on the scattering mechanism considered, and α is a prefactor denoting all non-energy dependent factors. Furthermore, before computing the transport properties, band gap is corrected to match the corresponding experimental values.[22]

The variation of Seebeck coefficient or thermopower, obtained within the constant relaxation time approximation, is plotted as a function of electron energy in Fig. 2. Thermopower with corrected band gap is on an average 10% higher than that without the correction, while the electron energy at which the thermopower is a maximum remains unaffected. Results also suggest that alloying has a much more favorable effect on thermopower than does heterostructuring. Additionally, the Lorenz number, $L=\kappa^e/\sigma T$ (which is a constant, $(\pi^2/3)(k_B/e)^2$ according to the Wiedemann-Franz law[23]), is found to increase with reduced electron energy or carrier concentration, and it equals $(\pi^2/3)(k_B/e)^2$ at electron energies higher than 0.5 eV. For all the heterostructures considered in this work, thermopower and Lorentz number are found to vary monotonically, similar to what is found for bulk semiconductors.[24]

It is noted that this contradicts the general conclusion of Bian *et al.*[13]—based on miniband calculations for InGaAs/

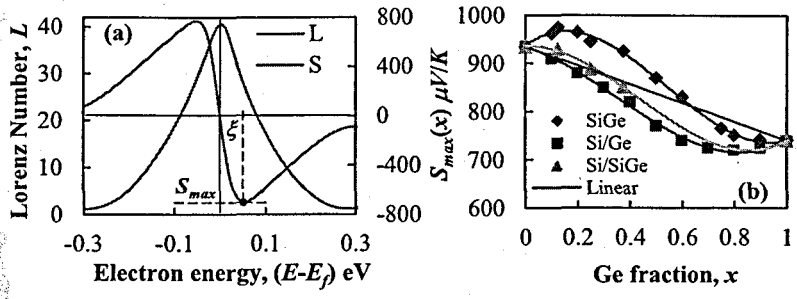

FIG. 2. (a) Variation of Lorenz number L and thermopower S as a function of the electron energy for a heterostructure configuration (Si/Ge) with Si:Ge = 3:3, under a constant relaxation time approximation. The compositional variation of the maximum thermopower $S_{max}(x)$ is shown for alloy configuration (marked by SiGe), heterostructure configuration (marked by Si/Ge), and alloy-heterostructure configuration (marked by SiGe) are shown in (b). The straight line represents a linear prediction for the compositional variation of thermopower.

InGaAlAs heterostructures—that S and L do not change monotonically for a superlattice. Although the miniband model was verified with experiments for a larger superlattice, oscillations were found in calculations for a short-period superlattice. Nonetheless, the discrepancy in qualitative behavior between DFT and miniband results for the short-period superlattice could originate from (1) material difference (Bian *et al.* dealt with InGaAs—a direct band gap material, and here we study SiGe—an indirect band gap material), or (2) modeling of band bending and electronic structure with approximations in the miniband calculations. In the miniband calculations, the Kronig-Penny model is used with a constant band potential for each element and a parabolic dispersion is assumed to compute charge distribution or band bending, while the effect of interfacial strain and corresponding band bending are completely ignored. For a short-period superlattice, band bending and charge distribution can deviate significantly from those in a larger superlattice.[25–29] While oscillatory behavior has yet to be clearly verified experimentally, Ishida *et al.*,[9] show with similar miniband calculations that a EuTe/PbTe short-period superlattice exhibits a monotonic behavior in the Seebeck coefficient, even for short-period superlattice. Thus, while contradictory information is reported for miniband calculations, *ab initio* calculations (which do not approximate the band dispersion and but do fully account for strain and disorder effects) do not support the conclusion that short-period superlattice S or L should exhibit oscillatory doping dependence,[13] underscoring the importance of an accurate description of electronic bands for transport calculations.

The Seebeck coefficient increases linearly at lower electron energy, and after reaching a maximum value, it decreases nonlinearly with a further increase in electron energy. For each alloy composition, represented by x, there is a maximum Seebeck coefficient, which we denote by $S_{max}(x)$, and the electron energy at which $S(x) = S_{max}(x)$ for a particular composition is denoted by the Greek symbol ξ. At 300 K, in silicon $S_{max}(x=0)$ is 930 μV/K and for Germanium $S_{max}(x=1.0)$ is 760 μV/K, both of which appear near an electron energy of 0.045 eV from the Fermi energy such that $\xi = 0.045$ eV. At the same temperature, results obtained with alloy ($Si_{1-x}Ge_x$) and heterostructure configurations (Si/Ge, and $Si/Si_{1-x}Ge_x$) show that the highest Seebeck coefficient among the three broadly classified configurations (Si/Ge, SiGe, and Si/SiGe) appears for the alloy configuration. Furthermore, over all the alloy configurations considered, the maximum thermopower $S_{max}(x)$ is obtained for a Ge fraction of 12.5% Ge in $Si_{1-x}Ge_x$, showing that $S_{max}(0.125) > S_{max}(x)$ with $x = \{0.0, 0.5, 0.75, 0.875, 1.0\}$. $S_{max}(x)$ for $Si_{0.5}Ge_{0.5}$ and Si/Ge are 870 μV/K and 770 μV/K, respectively, whereas for $Si/Si_{0.5}Ge_{0.5}$, $S_{max}(0.5)$ is estimated to be 800 μV/K.

Compositional variation of $S_{max}(x)$ is nonlinear for Si/Ge and SiGe, while for Si/SiGe, it follows mainly a linear variation. Compared to alloy configurations, the heterostructure configurations show a reduction in Seebeck coefficient. The reduction in thermopower for the nanostructure is due to a reduction in its value in the out-of-plane direction. Moreover, the length of the supercell—which is varied from 4 nm (6 unit cells) to 5.5 nm (10 unit cells) along the direction normal to the interface—is found to have negligible effect on the compositional dependence of $S_{max}(x)$. Electron energy relative to the Fermi energy ($E - E_f$) can however be converted to doping density using the relation, $p = 2(2\pi m^* k_B T/h^2)^{3/2} \exp[(E - E_f)/k_B T]$, for p-type doping, where p is the hole density, m^* (= 0.36 m_e for Si and 0.21 m_e for Ge) is the conductivity effective mass, h is Planck's constant (6.63×10^{-34} J-s), and $k_B T$ is the thermal energy (26 meV at 300 K). As calculation of the carrier density involves approximations to the conductivity effective masses, results are shown and discussed throughout this article in terms of electron energy.

In the SiGe systems studied, the most relevant scattering is the alloy scattering or acoustic phonon scattering or deformation potential scattering (which is proportional to $E^{-1/2}$), the non-polar optical phonon scattering (which is proportional to $E^{-3/2}$), or the ionized impurity scattering (which is proportional to $E^{3/2}$).[23] To examine the influence of relaxation time functions on transport coefficients, these energy dependent relaxation time functions are used in conjunction with a unique prefactor α, the determination of which

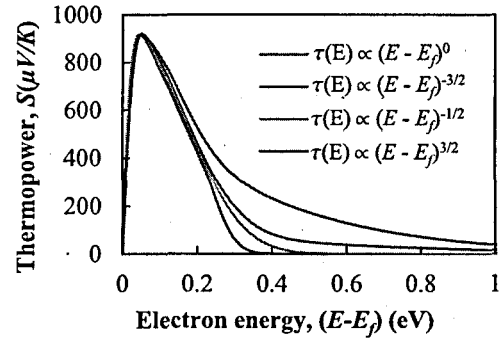

FIG. 3. Effect of energy dependent relaxation time functions on thermopower in Si. The thermopower in crystalline Si is a maximum for an electron energy of ~0.05 eV, which amounts to a doping level of 4×10^{19} (p-type), 2.5×10^{19} (Si n-type) cm^{-3}. Compared to constant RTA, ionized impurity scattering results in higher thermopower and non-polar optical phonon scattering and acoustic phonon scattering results in lower thermopower.

depends on the details of scattering and constitutes a separate rigorous study. Results shown in Fig. 3 indicate that the energy dependence of relaxation time affects transport properties mostly at higher electron energies, beyond 0.2 eV, which amounts to a high doping level of 5×10^{21} (Ge p-type), 1×10^{22} (Si p-type), 2.5×10^{21} (Ge n-type), or 8×10^{21} (Si n-type) cm^{-3}. For electron energies above 0.2 eV, scattering induced deviation from the constant RTA behavior is significant for the ionized impurity scattering. However, to analyze the role of composition and nanostructure formation on $S_{max}(x)$ and ξ (both of which are found to be unaffected by the energy dependence of the relaxation time), results obtained with the constant RTA are shown/discussed in the rest of the article. This also enables computing transport properties accurately, if the constant relaxation time for a configuration is known.

The effect of temperature on $S_{max}(x)$ and ξ is shown for 5 composition cases ($x = 0.0, 0.25, 0.5, 0.75, 1.0$) in Fig. 4, for the SiGe configuration. While $S_{max}(x)$ decreases rapidly with temperature, the electron energy or the doping level increases linearly with increasing temperature for all cases, except for $x = 0.75$, where it shows a nonlinear behavior. This composition is close to the crossover composition, $x = 0.85$, where the minimum of the conduction band switches its position from the ΓX direction to the ΓL direction. Moreover, alloying increases ξ for n-type doping or for $E\text{-}E_f > 0$ and decreases it for p-type doping or for $(E\text{-}E_f) < 0$. Nevertheless, the dependence of $S_{max}(x)$ on temperature exhibits identical behavior for both n-type doping and p-type doping.

At room temperature, ξ is closer to the Fermi-energy (only ~0.05 eV from E_f for $x = 0$, for example) and it shows weak dependence on composition. This is because of the narrower width of the carrier distribution at lower temperatures and the insignificant compositional variation of the density of states (DOS) in $Si_{1-x}Ge_x$ near the Fermi energy. This can be understood further based on the behavior of the components (the transmission function, the gradient of the Fermi-Dirac distribution function, and the energy dependent factor) of the integrands appearing in the equations for the transport coefficients. The gradient of the Fermi-Dirac distribution represented by Eq. (6) is always maximum at the Fermi-energy and it material independent. Thus, the dependence of the transport coefficients, represented by Eqs. (3)–(5), on material type or alloying arises solely from the transmission function, or Eq. (7), which involves material dependent relaxation time, group velocity, and DOS. Assuming comparable group velocities in SiGe (which is a reasonable assumption for SiGe at the start of conducting states or the initial portion of the DOS profile) and a constant relaxation time, the behavior of the transmission function can be understood by the DOS alone. The energy difference between the Fermi energy and the energy at which conducting electronic states appear is dictated by the band gap, which is also a material property. Considering the intrinsic Fermi energy level to lie at the middle of the band gap, the first electronic states become available for the electrons/holes for Si, for example, at $1.17/2 = 0.585$ eV (where 1.17 eV is the band gap of Si), which is much farther from 0.05 eV, where $S = S_{max}(300\,K)$ $\forall x$, and the differences originating from DOS or material variation are negligible.

Moreover, at room temperature at 0.1 eV from the Fermi energy, for example, the gradient of Fermi-Dirac distribution $\left(\frac{\partial f_0}{\partial E}\right)$ is only 10% of its maximum value: $\left(\frac{\partial f_0}{\partial E}\right)\Big|_{E-Ef=0.1\,eV} = 0.1 \times \left(\frac{\partial f_0}{\partial E}\right)\Big|_{E=E_f}$. Consequently, the product of the transmission function and $\left(\frac{\partial f_0}{\partial E}\right)$ becomes almost insensitive to alloying, due to the weaker coupling (originating from a larger energy separation) between the gradient and the DOS. Thus, the peak of the Seebeck coefficient around 0.05 eV from the Fermi energy appears at nearly the same electron energy ξ, regardless of the Ge fraction in the alloy. However, at higher temperatures, such as at 600 K, $(\frac{\partial f_0}{\partial E})|_{E-Ef=0.1eV} = 0.5 \times (\frac{\partial f_0}{\partial E})|_{E=E_f}$, indicating a widening of the gradient's profile. Therefore, at higher temperatures, the gradient profile broadens laterally (along the electron energy). As a

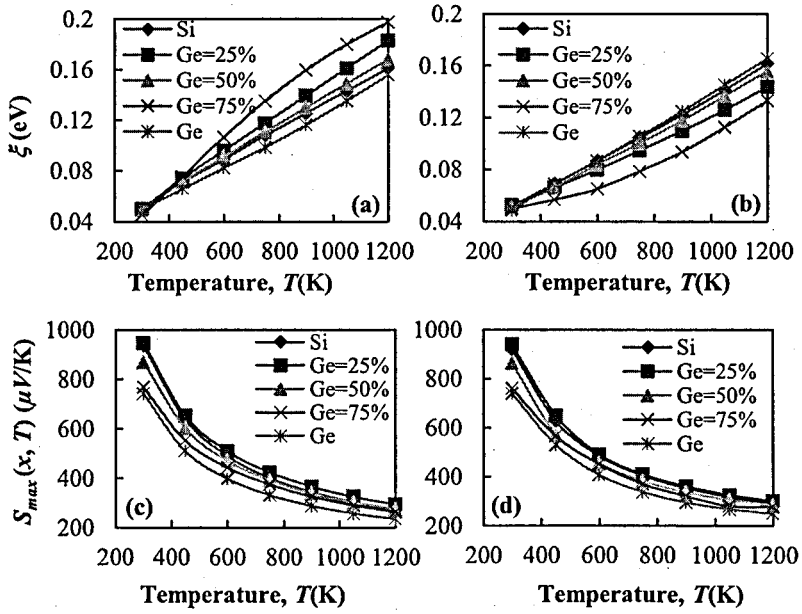

FIG. 4. Effect of temperature on the maximum thermopower $S_{max}(x)$ and the electron energy ξ, where $S(x) = S_{max}(x)$. Right (left) panels show temperature effects on the variation of the maximum thermopower, $S_{max}(x)$ and the corresponding electron energy, for electron energies smaller (higher) than the Fermi energy, indicating asymmetric behavior of ξ on two sides of the Fermi energy.

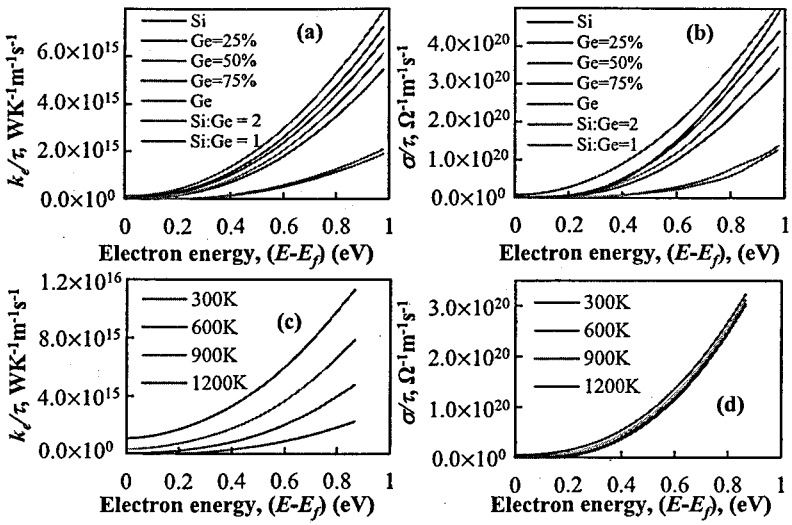

FIG. 5. Compositional variation of electrical conductivity and electron thermal conductivity in SiGe alloy and Si/Ge heterostructure. Layer thickness ratio does not show significant influence, particularly for lower electron energies. In the lower panel, the effect of temperature on conductivity is shown for $x = 0.5$ for the SiGe alloy configuration.

result, it couples with more electronic states and makes a stronger connection with the compositional variation, because integrated compositional or material variation has a stronger effect in the deeper conduction electronic states. Thus, compositional variation of the peak of the Seebeck coefficient becomes substantial and this coupling shifts ξ toward higher electron energies, as shown in Figs. 4(a) and 4(b).

Next, we explore the effects of alloying and nanostructuring on electron thermal conductivity and electrical conductivity, as shown in Fig. 5. Both the conductivities increase exponentially with respect to electron energy and are reduced by more than 50% by heterostructuring, which suggests that the reduction in total thermal conductivity (phonon thermal conductivity and electron thermal conductivity) is due to both electrons and phonons; however, phonon thermal conductivity is expected to dominate over the electron thermal conductivity. Temperature effects shown in Figs. 5(c) and 5(d) indicate that the percentage change in conductivity due to temperature is much higher for electron thermal conductivity than electrical conductivity. Both the conductivities increase with temperature. The increase in electron thermal conductivity due to temperature is pronounced at higher electron energies, suggesting stronger temperature sensitivity of the electron thermal conductivity at higher doping density. So, with respect to the thermal effect on electron transport, highly doped SiGe would exhibit a significant reduction in ZT at higher temperatures due to a substantial reduction in thermopower and an increase in electron thermal conductivity.

In conclusion, the effects of heterostructuring and alloying on electron dependent transport properties are quantified and comprehensively studied for a range of SiGe systems. Of the configurations examined, results show that thermopower, electrical thermal conductivity, and electrical conductivity are reduced by heterostructuring. The highest observed thermopower, $S_{max}(x)$, is found to occur at $x = 0.125$ for the alloy configuration. While enhancement in thermoelectric properties due to a reduction in thermal conductivity alone is reported for a wide composition range, our results suggest that in some cases lower Ge fraction would offer advantages over higher Ge fraction, due solely to the improved electron dependent transport properties. Consequently, alloying offers greater potential than short-period heterostructuring for enhancing thermopower. We also show that the energy dependent relaxation time affects thermopower only at a high doping level, and both Seebeck coefficient and Lorenz number vary without showing any surprising oscillations in heterostructure configuration.

[1]G. D. Mahan and J. O. Sofo, Proc. Natl. Acad. Sci. U.S.A. **93**, 7436 (1996).
[2]F. J. DiSalvo, Science **285**, 703 (1999).
[3]A. Majumder, Science **303**, 777 (2004).
[4]G. J. Snyder and E. S. Toberer, Nature Mater **7**, 105 (2008).
[5]D. G. Cahill, W. K. Ford, K. E. Goodson, G. D. Mahan, A. Majumdar, H. J. Maris, R. Merlin, and S. R. Phillpot, J. Appl. Phys. **93**, 793 (2003).
[6]A. I. Boukai, Y. Bunimovich, J. Tahir-Kheli, J. K. Yu, W. A. Goddard III, and J. R. Heath, Nature **451**, 168 (2008).
[7]D. Li, S. T. Huxtable, A. R. Abramson, and A. Majumdar, J. Heat Transfer **127**, 108 (2005).
[8]X. W. Wang, H. Lee, Y. C. Lan, G. H. Zhu, G. Joshi, D. Z. Wang, J. Yang, A. J. Muto, M. Y. Tang, J. Klatsky, S. Song, M. S. Dresselhaus, G. Chen, and Z. F. Ren, Appl. Phys. Lett. **93**, 193121 (2008).
[9]A. Ishida, D. Cao, S. Morioka, M. Veis, Y. Inoue, and T. Kita, Appl. Phys. Lett. **92**, 182105 (2008).
[10]J.-H. Lee, J. Wu, and J. C. Grossman, Phys. Rev. Lett. **104**, 016602 (2010).
[11]C. Jeong, R. Kim, M. Luisier, S. Datta, and M. Lundstrom, J. Appl. Phys. **107**, 023707 (2010).
[12]P. Pichanusakorn and P. R. Bandaru, Appl. Phys. Lett. **94**, 223108 (2009).
[13]Z. Bian, M. Zebarjadi, R. Singh, Y. Ezzahri, A. Shakouri, G. Zeng, J. H. Bahk, J. Bowers, J. Zide, and A. Gossard, Phys. Rev. B **76**, 205311 (2007).
[14]D. Vashaee, Y. Zhang, A. Shakouri, G. Zeng, and Y.-L. Chiu, Phys. Rev. B **74**, 195315 (2006).
[15]L. W. Whitlow and T. Hirano, J. Appl. Phys. **78**, 5460 (1995).
[16]Z. Tao and L. Friedman, J. Phys. C **18**, L455 (1985).
[17]K. Ahn, E. Cho, J.-S. Rhyee, S. Il Kim, S. M. Lee, and K. H. Lee, Appl. Phys. Lett. **99**, 102110 (2011).
[18]D. Bilc and P. Ghosez, Phys. Rev. B **83**, 205204 (2011).
[19]Y. Zhang, X. Ke, C. Chen, J. Yang, and P. Kent, Phys. Rev. Lett. **106**, 206601 (2011).
[20]J. M. Soler, E. Artacho, J. D. Gale, A. Garcia, J. Junquera, P. Ordejon, and D. Sanchez-Portal, J. Phys.: Condens. Matter **14**, 2745 (2002).
[21]G. K. H. Madsen and D. J. Singh, Comput. Phys. Commun. **175**(1), 67 (2006).
[22]R. People, Phys. Rev. B **32**, 1405 (1985).
[23]N. W. Ashcroft and N. D. Mermin, Solid State Physics (Saunders College Publishing, 1976).
[24]G. S. Kumar, G. Prasad, and R. O. Pohl, J. Mater. Sci. **28**, 4261 (1993).
[25]M. Peressi, N. Binggeli, and A. Baldereschi, J. Phys. D: App. Phys. **31**, 1273 (1998).
[26]S. S. Li, *Semiconductor Physical Electronics* (Springer, 2006).
[27]R. T. Tung, Mater. Sci. Eng. R **35**, 1 (2001).
[28]A. Baldereschi, S. Baroni, and R. Resta, Phys. Rev. Lett. **8**, 734 (1988).
[29]A. Stroppa and M. Peressi, Phys. Rev. B **71**, 205303 (2005).